pubs.acs.org/Biomac

Article

Substrate Engineering in Lipase-Catalyzed Selective Polymerization of D-/L-Aspartates and Diols to Prepare Helical Chiral Polyester

Yu Zhang,[§] Bo Xia,*[,§] Yanyan Li, Xianfu Lin, and Qi Wu*

Cite This: *Biomacromolecules* 2021, 22, 918–926

Read Online

ACCESS | Metrics & More | Article Recommendations | Supporting Information

ABSTRACT: The synthesis of optically pure polymers is one of the most challenging tasks in polymer chemistry. Herein, Novozym 435 (Lipase B from *Candida antarctica*, immobilized on Lewatit VP OC 1600)-catalyzed polycondensation between D-/L-aspartic acid (Asp) diester and diols for the preparation of helical chiral polyesters was reported. Compared with D-Asp diesters, the fast-reacting L-Asp diesters easily reacted with diols to provide a series of chiral polyesters containing *N*-substitutional L-Asp repeating units. Besides amino acid configuration, *N*-substituent side chains and the chain length of diols were also investigated and optimized. It was found that bulky acyl *N*-substitutional groups like *N*-Boc and *N*-Cbz were more favorable for this polymerization than small ones probably due to competitively binding of these small acyl groups into the active site of Novozym 435. The highest molecular weight can reach up to 39.5×10^3 g/mol (M_w, $Đ = 1.64$). Moreover, the slow-reacting D-Asp diesters were also successfully polymerized by modifying the substrate structure to create a "nonchiral" condensation environment artificially. These enantiocomplementary chiral polyesters are thermally stable and have specific helical structures, which was confirmed by circular dichroism (CD) spectra, scanning electron microscope (SEM), and molecular calculation.

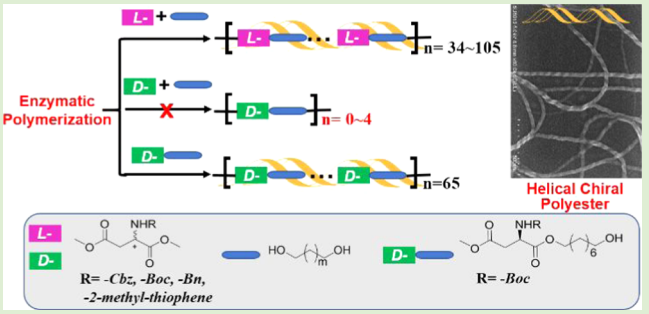

INTRODUCTION

Many naturally occurring polymers, such as polysaccharides, proteins, and nucleic acids, possess specific chiral structure, and play key roles in biological systems, for example, molecular recognition and catalytic activity. Similarly, the stereochemistry of synthetic chiral polymers often markedly influences their physical and chemical properties.[1] As a result, in polymer chemistry, the synthesis of optically pure polymers has been one of the most challenging tasks. Generally, both chemical and biocatalytic routes can be applied for the preparation of optically pure polymers. In comparison with traditional chemical routes that usually use metal-based chiral catalysts with complex structures and relatively harsh reaction conditions,[2] biocatalysts from natural sources such as lipase are an important extension in the quest to procure optically pure polymers due to their green and highly selective specialty.[3]

For the last 2 decades, many developments concerning lipase-catalyzed synthesis of polyesters via polycondensation of diacids and diols (or hydroxy acids), and ring-opening polymerization (ROP) of lactones, have been achieved. For such lipase-catalyzed polymerization, the acyl of diacids (or diester, hydroxy acids, and lactones) combines with the active sites of lipase to form an "acyl−enzyme" complex. Then, the hydroxyl of appropriate configurational diols (or hydroxy acids) attacks the "acyl−enzyme complex" to perform transesterification providing dimers and the enzyme is released. The repeat of this process provides targeting polymers.[4] However, most of these polyesters reported are achiral or racemic. The introduction of chirality into polyesters may provide superior properties relative to achiral polyesters or modulate their chemical and physical properties.[5,6] For example, by introducing chirality in poly-(4-methylcaprolatone), the degradation rate can be tuned.[7] As pointed above, the key process of lipase-catalyzed polymerization was the transesterification between appropriate configurational diols and the acyl−enzyme complex. And according to Kazlauskas's rule,[8] most lipases showed a high preference for (*R*)-configured secondary alcohols in the process of enzymatic acylation. Thus, lipase-catalyzed polymerization was not suitable for polycondensation of racemic diols and dicarboxylic acid derivatives because the extremely low reactivity of the hydroxy groups at the (*S*)-configured alcohol limited chain growth by acting as chain stoppers. A similar problem was observed in the Novozym 435-catalyzed ROP of 6-alkyl caprolactones such as 6-methylcaprolactone (6-MeCL),

Received: November 11, 2020
Revised: December 19, 2020
Published: January 11, 2021

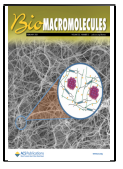

https://dx.doi.org/10.1021/acs.biomac.0c01605
Biomacromolecules 2021, 22, 918–926

because the Novozym 435-catalyzed selective ring-opening product of 6-MeCL is a terminal secondary alcohol with (*S*)-configuration, the slow-reacting enantiomer for Novozym 435. Meijer and Heise proposed a potential solution for ROP of 6-MeCL and polycondensation of racemic diols and dicarboxylic acid derivatives, respectively, namely, dynamic kinetic resolution (DKR) polymerization of racemic monomers by coupling ruthenium-catalyzed racemization of the terminal *S*-enantiomers of the propagating polymer.[9] However, in some cases, only low-molecular-weight oligomers were obtained (degree of polymerization 3−5 for ring-opening polymerization[10] and M_w were 3.4×10^3 g/mol for polycondensation[11]), and a further improvement in the molecular weight of chiral polyesters is still needed. It is therefore far more desirable to design a synthetic strategy for improving the molecular weight of optically pure polyesters.

Generally, L-amino acids are abundant in nature, and to date, two enantiomers of many α-amino acids are highly commercially available. Especially, some amino acids such as aspartic acid (Asp) and glutamic acid (Glu) have two acid groups and suit to be incorporated into the backbone of chiral polyester as diacids monomers. Additionally, the NH_2 of Asp or Glu can facilely introduce functional groups into the traditional polyesters. Moreover, using optically pure amino acids as monomers in enzymatic polymerization, both high molecular weight and high optical purity of the targeting chiral polyesters can be achieved simultaneously. Thus, amino acid enantiomers probably are an important alternative to racemic monomers for preparing high-molecular-weight chiral polyesters. In our primary studies, we found that the Novozym 435-catalyzed polycondensation between racemic Asp diesters and achiral diols was not successful, because Novozym 435 showed a high preference for L-Asp diesters and the chain growth reaction was stopped when slow-reacting D-Asp diesters locating at the chain terminal. This problem was similar to that one observed in Novozym 435-catalyzed ROP of 6-MeCL and polycondensation of racemic diols and dicarboxylic acid derivatives.[10,11] However, the strategy proposed by Meijer and Heise was not efficient in this case because of the difficult racemization of general racemic acid derivatives without the α-electron-withdrawing group.[12] Herein, this paper reports Novozym 435-catalyzed preparation of various chiral polyesters with high optical purity and high molecular weight starting from diols and L- or D-Asp diesters with different *N*-substituents. The highest molecular weight can reach up to 39.5×10^3 g/mol (M_w). The influence of substrate structure, including amino acid configuration, *N*-substituent side chain, and the chain length of diols, were investigated in detail. This work also demonstrated how limitations of the selectivity of this lipase for the slow-reacting D-Asp diesters were solved using substrate engineering strategy, i.e., modifying D-Asp diester structure to hide the chiral centers and create a "nonchiral" condensation environment artificially, thus chiral polyesters of D-Asp with high molecular weight were also prepared successfully.

EXPERIMENTAL SECTION

Materials. The L- and D- aspartic acids are commercially available and purchased from Bidepharm. Sigma-Aldrich offered the Lipase B from *Candida antarctica* (Novozym 435). Other reagents and compounds were supported by Aladdin.

Methods. The structures of both monomers and polymers were characterized by nuclear magnetic resonance (NMR). Tetramethylsilane (TMS) was added as the internal standard during the ^{1}H NMR and ^{13}C NMR tests. The Bruker AMX-400 MHz spectrometer (Rheinstetten, Germany) was adopted using $CDCl_3$ as solvents.

The thermal properties of polymers were characterized with differential scanning calorimetry (DSC). A DSCQ1000 TA Instrument, with the calorimeter under a nitrogen atmosphere (30 mL/min) connected to a cryostat from the same manufacturer, was adopted for these tests. The samples were prepared in crimped aluminum pans. The standard procedure was conducted with a heating rate of 10 °C/min from −50 to 100 °C.

The molecular weight of polymers was determined by size exclusion chromatography (SEC) with a system equipped with a refractive-index detector (Waters 2414) and Waters Styragel SEC columns (Massachusetts). The SEC columns were standardized with narrow-dispersity polystyrene in molecular weight ranging from 6×10^5 to 500 g/mol. Tetrahydrofuran (THF) was used as the mobile phase with a flow rate of 1.0 mL/min, the concentration of the sample is 3.0 mg/mL.

Circular dichroism (CD), recorded on a JASCO J-815 spectrometer, was used for the configuration's determination of chiral polymers. The light path length of the quartz cell used was 10 mm. Acetonitrile was used as the solvent and the concentration was about 0.01 mg/mL.

Scanning electron microscopy (SEM) measurement were performed as follows. Polymers were dissolved in dichloromethane, then *n*-hexane was added to this solution. Samples were prepared by loading 2.0 μL of the polymer solution in dichloromethane/*n*-hexane onto a silicon slice. After drying overnight, the samples were sputtered with gold for 90 s and measured by SEM on a Hitachi S-4800 with an accelerating voltage of 3.0 kV.

The theoretical simulation had been performed to optimize the compounds L-**9a**, **poly**(L-**9a**) chain, and the **poly**(L-**9a**) helix microstructure using Molecular Mechanics methods with universal force field (UFF) by the Gaussian 09 Linux program package on a Dell Power Edge R720 computer with nineteen XEON(R) E5-2620 CPUs @2.00 GHz. The stabilization energies (E_{stable}) for the helix microstructure were calculated using the following equation: $E_{stable} = E_{helix} - [E_{chain} + E_{chain}]$. E_{helix} was the total energy of the **poly**(L-**9a**) helix microstructure including two **poly**(L-**9a**) chains, whereas the E_{chain} is the total energies of the **poly**(L-**9a**) chain. The optimized compound structures were visualized using GaussView 05 program.

Synthesis Procedure of Monomers. *Synthesis of L-1 and L-10.* Two milliliter of thionyl chloride was added into 50 mL of methanol solution containing *N*-Cbz amino acid (5.0 g). Then, the reaction mixture was refluxed overnight and concentrated in vacuum. The obtained crude product was used for next polymerization without any purification.

Dimethyl N-Cbz-L-aspartate (L-1). ^{1}H NMR (400 MHz, $CDCl_3$) δ: 7.26 (m, 5H), 5.05 (s, 2H), 4.57 (m, 1H), 3.69 (s, 3H), 3.61 (s, 3H), 2.88 (m, 2H) ppm. ^{13}C NMR (100 MHz, $CDCl_3$) δ: 171.4, 171.2, 155.9, 136.1, 128.6, 128.3, 128.1, 67.2, 52.9, 52.1, 50.3, 36.5 ppm.

Dimethyl N-Cbz-L-glutamate (L-10). ^{1}H NMR (400 MHz, $CDCl_3$) δ: 7.29 (m, 5H), 5.04 (s, 2 H), 4.36 (m, 1H), 3.69 (s, 1H), 3.59 (s, 1H), 2.33 (m, 2H), 2.15 (m, 1H), 1.93 (m, 1H) ppm. ^{13}C NMR (100 MHz, $CDCl_3$) δ: 173.2, 172.3, 155.9, 136.1, 128.6, 128.2, 128.1, 67.1, 53.3, 52.6, 51.9, 30.0, 27.6 ppm.

Synthesis of L-2 and L-3. Five milliliter of thionyl chloride was added into 50 mL of methyl alcohol solution containing aspartic acid (0.5 mmol). Then, the mixture was refluxed overnight and concentrated in vacuum to obtain the dimethyl aspartate hydrochloride. The crude product was used without any purification.

Aspartic acid dimethyl esters (30 mmol) were dissolved in 80 mL of dichloromethane. Aldehydes (33 mmol) and sodium borohydride (46 mmol) were added, and the mixture was stirred at room temperature for 24 h. The reaction was quenched by addition of saturated ammonium chloride. After stirring for 30 min, 10% NaOH was added to bring the solution to pH = 10. Then, the mixture was extracted with dichloromethane (50 mL × 3). The combined organic layer was dried over $MgSO_4$, filtered, and concentrated. The crude

https://dx.doi.org/10.1021/acs.biomac.0c01605
Biomacromolecules 2021, 22, 918−926

product was purified by column chromatography eluting with 50% acetone/hexanes to give the product as a yellow oil in 85% yield. The NMR of *N*-functionalization-D-amino acid diesters were the same as *N*-functionalization-L-amino acid diesters.

*Dimethyl N-Benzyl-L-aspartate (L-**2**).* ^{1}H NMR (400 MHz, $CDCl_3$) δ: 7.32−7.25 (m, 5H), 3.90−3.87 (d, 1H, J = 12.8), 3.74 (s, 3H), 3.72−3.68 (d, 1H, J = 24 Hz), 3.68 (s, 3H), 3.67−3.65 (m, 1H), 2.74−70 (m, 2H), 1.87 (brs, 1H) ppm. ^{13}C NMR (100 MHz, $CDCl_3$) δ: 174.1,171.3, 139.5, 128.4, 128.3, 127.2, 56.9, 52.2, 52.0, 51.9, 38.0 ppm.

*Dimethyl N-(Thiophen-2-ylmethyl)-L-aspartate (L-**3**).* ^{1}H NMR (400 MHz, $CDCl_3$) δ: 7.15−7.14 (m, 1H), 6.88−6.86 (m, 2H), 4.05−3.86 (m, 2H), 3.68 (s, 3H), 3.64−3.61 (d, 1H, J = 12 Hz), 3.62 (s, 3H), 2.68 (m, 2H), 2.21 (brs, 1H) ppm. ^{13}C NMR (100 MHz, $CDCl_3$) δ: 173.9, 171.3, 143.3, 126.6, 125.2, 124.8, 56.3, 52.2, 51.9, 46.7, 38.0 ppm.

*Synthesis of L-**4** to L-**9**.* Aspartic acid diester (1.0 equiv) was dissolved in dichloromethane. Then, anhydride (1.1 equiv), DMAP (10%, wt % of the ester), and tetraethylammonium (TEA) (2.0 equiv) were added to this solution and stirred overnight at room temperature (RT). After the reaction was complete as verified by thin-layer chromatography (TLC) (petroleum ether/ethyl acetate = 3:1), the mixture was washed with.0 M HCl and saturated $NaHCO_3$ solution. The obtained organic solution was dried over $MgSO_4$ and concentrated in vacuum to get the crude product. The crude product was used for further polymerization without any purification.

*Diethyl N-Propionyl-L-aspartate (L-**4**).* ^{1}H NMR (400 MHz, $CDCl_3$), δ: 6.64−6.62 (m, 1H), 4.74−4.72 (m, 1H), 40.9−4.01 (m, 4H), 2.85−2.69 (m, 2H), 2.16−2.14 (m, 2H), 1.16−1.01 (m, 9H) ppm; ^{13}C NMR (100 MHz, $CDCl_3$), δ: 172.67, 170.04, 169.93, 60.73, 59.94, 52.59, 47.51, 35.40, 28.35, 13.10, 13.05, 8.62 ppm.

*Dimethyl N-Hexanoyl-L-aspartate (L-**5**).* ^{1}H NMR (400 MHz, $CDCl_3$), δ: 6.51−6.49 (brs, 1H), 4.90−4.86 (m, 1H), 3.77 (s, 3H), 3.70 (s, 3H), 3.07−3.01 (dd, 1H, J = 4 Hz), 2.89−2.85 (dd, 1H, J = 4 Hz), 2.25−2.21 (m, 2H), 1.66−1.62 (m, 2H), 1.32−1.31 (m, 4H), 0.91−0.88 (t, 3H, J = 12 Hz) ppm; ^{13}C NMR (100 MHz, $CDCl_3$), δ: 172.9, 171.7, 171.3, 52.8, 52.0, 48.3, 36.4, 36.1, 31.3, 25.2, 22.4, 13.9 ppm.

*Diethyl N-(2,2,2-Trifluoroacetyl)-L-aspartate (L-**6**).* ^{1}H NMR (400 MHz, $CDCl_3$) δ: 7.37−7.36 (brs, 1H), 4.76−4.72 (m, 1H), 4.21−4.17 (m, 2H), 4.13−4.08 (m, 2H), 3.07−2.79 (m, 2H), 1.24−1.18 (m, 6H) ppm; ^{13}C NMR (100 MHz, $CDCl_3$) δ: 169.6, 168.0, 156.1, 155.7, 116.0, 113.1, 61.6, 60.5, 47.9, 34.4, 13.0, 12.9 ppm.

*Dimethyl N-Isobutyryl-L-aspartate (L-**7**).* ^{1}H NMR (400 MHz, $CDCl_3$), δ: 6.51−6.49 (brs, 1H), 4.89−4.84 (m, 1H), 3.77 (s, 3H), 3.70 (s, 3H), 3.06−2.88 (dd, 1H, J = 4 Hz), 2.88−2.83 (dd, 1H, J = 4 Hz), 2.44−2.39 (m, 1H), 1.19−1.15 (t, 6H, J = 16 Hz) ppm; ^{13}C NMR (100 MHz, $CDCl_3$), δ: 176.7, 171.7, 171.4, 52.8, 52.0, 48.2, 36.1, 35.4, 19.4, 19.3 ppm.

*Dimethyl N-Pivaloyl-L-aspartate (L-**8**).* ^{1}H NMR (400 MHz, $CDCl_3$) δ: 6.73−6.71 (brs, 1H), 4.86−4.52 (m, 1 H), 3.77 (s, 3H), 3.70 (s, 3H), 3.06−3.00 (dd, 1H, J = 4 Hz), 2.87−2.82 (dd, 1H, J = 4 Hz), 1.22 (s, 9H); ^{13}C NMR (100 MHz, $CDCl_3$) δ: 178.3, 171.7, 171.5, 52.8, 52.0, 48.4, 38.7, 35.9, 27.3, 26.5 ppm.

*Dimethyl N-(Tert-butoxycarbonyl)-L-aspartate (L-**9**).* ^{1}H NMR (400 MHz, $CDCl_3$) δ: 5.45−5.43 (brs, 1H), 4.52−4.50 (m, 1H), 3.69 (s, 3H), 3.63 (s, 3H), 2.97−2.92 (dd, 1H, J = 4 Hz), 2.78−2.73 (dd, 1H, J = 4 Hz), 1.38 (s, 9H) ppm; ^{13}C NMR (100 MHz, $CDCl_3$) δ: 170.5, 155.8, 154.4, 51.7, 32.9, 27.3, 27.0, 24.6, 23.9 ppm.

*Synthesis of D-**11** to D-**12**.*[2] 1,8-Octane-diol (15 mmol), dimethylaminopyridine (DMAP, 1.0 mmol), and dicyclohexylcarbodiimide (DCC, 10 mmol) were added into a solution of 20 mL of dichloromethane containing *N*-Boc-D-β-methyl-aspartate (10 mmol) or *N*-Boc-D-α-methyl-aspartate (10 mmol). Then, the reaction mixture was stirred overnight at 40 °C and TLC (petroleum ether/ethyl acetate = 3:1) was used to monitor the reaction progress. After the reaction completed, the mixture was washed with 5% $NaHCO_3$ and 5% citric acid. The organic phase was dried over $MgSO_4$ and concentrated in vacuum. The residue was purified with column chromatography (petroleum ether/ethyl acetate = 5:1).

*N-Boc-D-α-octanediol-β-methyl-aspartate (D-**11**).* ^{1}H NMR (400 MHz, $CDCl_3$) δ: 5.51−5.49 (m, 1H), 4.57−4.55 (m, 1 H), 4.17−4.11 (m, 2H), 3.69 (s, 3H), 3.66−3.63 (t, 2H, J = 12 Hz), 3.04−2.2.79 (m, 2H), 1.63−1.53 (m, 4H), 1.45 (s, 9H), 1.33−1.28 (m, 8H) ppm; ^{13}C NMR (100 MHz, $CDCl_3$) δ: 171.16, 171.11, 155.43, 80.09, 65.9, 63.0, 52.0, 50.0, 36.7, 32.7, 29.2, 29.1, 28.4, 28.3, 26.7, 25.6 ppm.

*N-Boc-D-α-methyl-β-octanediol-aspartate (D-**12**).* ^{1}H NMR (400 MHz, $CDCl_3$) δ: 5.55−5.53 (m, 1H), 4.58−4.56 (m, 1H), 4.10−4.07 (t, 2H, J = 12 Hz), 3.65−3.62 (t, 2H, J = 12 Hz), 2.98−2.79 (m, 2H), 1.63−1.55 (m, 4H), 1.45 (s, 9H), 1.37−1.33 (m, 8H) ppm; ^{13}C NMR (100 MHz, $CDCl_3$) δ: 171.65, 171.06, 155.42, 80.17, 65.18, 62.89, 52.71, 49.93, 36.83, 32.66, 29.22, 29.10, 28.43, 28.28, 25.72, 25.61 ppm.

Enzymatic Polymerization of Diesters and Diols. Diols (0.2 mmol) and Novozym 435 (15%, wt of monomers) were added into the solution of diesters (0.2 mmol) in 3.0 mL of toluene. Then, the flask was replaced under a nitrogen atmosphere and the reaction mixture was prepolymerized at 80 °C for 3 days. The mixture was concentrated in vacuum to remove the solvent and then reacted in vacuum for another 2 days (0.01 MPa). The obtained polymers were dissolved in 1.0 mL of chloroform. Then, 5.0 mL of petroleum ether (60−90 °C) was added slowly. After 10 min standing, the supernatant was discarded, and this procedure was repeated with the residue for 3 times. The final obtained polymers were concentrated in vacuum.

The polymerization of D-**11** and D-**12** was under the same reaction conditions (without the addition of diols) as the polymerization of diesters and diols.

*Poly(N-Cbz-L-asp-(1,8-octanediol)) Ester, Poly(L-**1a**).* SEC data: M_w = 39.5 × 10^3 g/mol, $Đ$ = 1.64; ^{1}H NMR (400 MHz, $CDCl_3$), δ: 7.29−7.19 (m, 5H), 5.73−5.71 (d, 1H, J = 8 Hz), 5.04 (s, 2H), 4.55−4.53 (m, 1H), 4.06−3.97 (m, 4H), 2.91−2.78 (m, 2H), 1.58−1.52 (m, 4H), 1.22 (s, 8H) ppm.

*Poly(N-Cbz-L-asp-(1,4-butanediol)) Ester, Poly(L-**1c**).* SEC data: M_w = 9.8 × 10^3 g/mol, $Đ$ = 1.29; ^{1}H NMR (400 MHz, $CDCl_3$), δ: 7.34−7.30 (m, 5H), 5.84 (s, 1H), 5.11 (s, 2H), 4.63−4.61 (m, 1H), 4.15−4.07 (m, 4H), 3.01−2.81 (m, 2H), 1.65 (s, 4H) ppm.

*Poly(N-Cbz-L-asp-(1,6-hexanediol)) Ester, Poly(L-**1d**).* SEC data: M_w = 12.8 × 10^3 g/mol, $Đ$ = 1.29; ^{1}H NMR (400 MHz, $CDCl_3$), δ: 7.36−7.31 (m, 5H), 5.82 (s, 1 H), 5.12 (s, 2 H), 4.63−4.61 (m, 1H), 4.14−4.04 (m, 4H), 3.03−2.81 (m, 2H), 1.61−1.59 (m, 4H), 1.33−1.26 (m, 4H).

*Poly(N-Cbz-L-asp-(1,12-dodecanediol)) Ester, Poly(L-**1e**).* SEC data: M_w = 16.9 × 10^3 g/mol, $Đ$ = 1.45; ^{1}H NMR (400 MHz, $CDCl_3$), δ: 7.37−7.32 (m, 5H), 5.79−5.77 (m, 1H), 5.12 (s, 2H), 4.63−4.61 (m, 1H), 4.14−4.04 (m, 4H), 1.62−1.58 (m, 4H), 1.28−1.28 (m, 16H).

*Poly(N-Bn-L-asp-(1,8-octanediol)) Ester, Poly(L-**2a**).* SEC data: M_w = 12.1 × 10^3 g/mol, $Đ$ = 1.49; ^{1}H NMR (400 MHz, $CDCl_3$), δ: 7.24−7.23 (m, 5H), 4.13−3.97 (m, 4H), 3.82−3.79 (d, 2H, J = 12), 3.66−3.63 (d, 2H, J = 12), 3.60−3.57 (m, 1H), 2.69−2.55 (m, 2H), 1.56−153 (m, 4H), 1.25−1.22 (m, 8H) ppm.

*Poly(N-Thiophene-2-ylmethyl-L-Asp-(1,8-octanediol)) Ester, **Poly**(L-**3a**).* SEC data: M_w = 11.4 × 10^3 g/mol, $Đ$ = 1.52; ^{1}H NMR (400 MHz, $CDCl_3$), δ: 7.20−7.19 (m, 1H), 6.93−6.91 (m, 2H), 4.14−3.92 (m, 6H), 3.69−3.62 (m, 1H), 2.77−2.64 (m, 2H), 1.63−1.60 (m, 4H), 1.31−1.25 (m, 8H) ppm.

*Poly(N-Boc-L-asp-(1,8-octanediol)) Ester, **Poly**(L-**9a**).* SEC data: M_w = 14.7 × 10^3 g/mol, $Đ$ = 1.62; ^{1}H NMR (400 MHz, $CDCl_3$), δ: 5.50−5.48 (d, 1H, J = 8 Hz), 4.56−4.51 (m, 1H), 4.14−4.05 (m, 4H), 3.00−2.77 (m, 2H), 1.62−1.58 (m, 4H), 1.44 (s, 9H), 1.30−1.24 (s, 8H) ppm.

*Poly(N-Cbz-L-glu-(1,8-octanediol)) Ester, Poly(L-**10a**).* SEC data: M_w = 19.3 × 10^3 g/mol, $Đ$ = 1.44; ^{1}H NMR (400 MHz, $CDCl_3$), δ: 7.35−7.32 (m, 5H), 5.48 (brs, 1H), 5.09 (s, 2H), 4.41−4.36 (m, 1H), 4.14−4.02 (m, 4H), 2.42−2.36 (m, 2H), 2.23−1.93 (m, 2H), 1.68−1.57 (m, 4H), 1.30 (s, 8H) ppm.

*Poly(N-Boc-D-asp-(1,8-octanediol)) Ester, Poly(D-**9a**).* SEC data: M_w = 23.1 × 10^3 g/mol, $Đ$ = 2.09; ^{1}H NMR (400 MHz, $CDCl_3$), δ: 5.50−5.48 (d, 1H, J = 8 Hz), 4.56−4.51 (m, 1H), 4.14−4.05 (m, 4H),

https://dx.doi.org/10.1021/acs.biomac.0c01605
Biomacromolecules 2021, 22, 918−926

3.00−2.77 (m, 2H), 1.62−1.58 (m, 4H), 1.44 (s, 9H), 1.30−1.24 (s, 8H) ppm.

RESULTS AND DISCUSSION

Novozym 435, which performed high stereo- and regioselectivity, was widely used in the kinetic resolutions and steric polymerizations.[13] Herein, it was the first choice for the steric selective polymerization of Asp diester and diols. As our previous study indicated that the preferential product of Novozym 435-catalyzed polycondensation between Asp diester and diols is polyamide due to the higher nucleophilicity of $-NH_2$ than hydroxyls,[14] the $-NH_2$-substituted dimethyl aspartate was applied for preparing the chiral polyesters. For testing the stereoselectivity of Novozym 435, D-, racemic D-/L- and L- Asp monomers were investigated, and the results are listed in Table 1 (entries 1, 5, and 8). According to the investigation, the L-Asp diester successfully provided poly(*N*-Cbz-L-Asp-(1,8-octanediol)) ester with a molecular weight up to 39.5 × 10^3 g/mol (M_w) and 76% yield, while the polycondensation of D-Asp diester was not successful (entry 1 vs entry 8, Table 1). It implied that Novozym 435 had a higher preference for L-*N*-Cbz-Asp $(OMe)_2$ than D- and racemic D-/L- *N*-Cbz-Asp $(OMe)_2$. The structure of the targeting polyester was confirmed by NMR, as shown in the Supporting Information. To further evaluate the influence of D-Asp enantiomer on the Novozym 435-catalyzed polycondensation, we attempted to change the L- and D-enantiomer ratio in the starting monomers (entries 2−7, Table 1). Initially, we added 1 percent of D-enantiomer in the L-enantiomer. And we found that the molecular weight of obtained polyester changed little (39.5 × 10^3 g/mol for pure L-monomer vs 41.0 × 10^3 g/mol for 1 percent D-monomer in L- monomer, entry 1 vs entry 2). However, when the ratio of L-/D-Asp diesters changed from 100:1 to 1:20, a continuous decrease of molecular weight and yields of polyesters was observed. And the monomer with a 1:20 ratio of L-/D-Asp diesters acted similarly as the pure D-Asp, whose polycondensation was also failed (entries 7−8, Table 1). The racemic *N*-Cbz-Asp $(OMe)_2$ only gave the targeting polyester with moderate molecular weight (entry 5, Table 1). These results clearly implied the negative effect of D-Asp enantiomer on this polycondensation and indicated that Novozym 435 had a higher preference for L-*N*-Cbz-Asp-$(OMe)_2$ than D-*N*-Cbz-Asp$(OMe)_2$.

Table 1. Polymerization of D-/L-Asp Diesters and Octanediol[a,b]

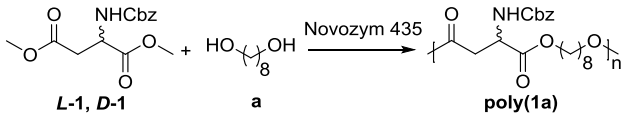

L-1, *D*-1 a poly(1a)

entry	L-/D-	M_w (×10^3 g/mol)	Đ	DP[c]	yield (%)
1	1:0	39.5	1.64	105	76
2	100:1	41.0	1.29	109	60
3	20:1	19.3	1.29	51	33
4	5:1	19.5	1.64	52	35
5	1:1	10.8	1.45	29	34
6	1:5	6.7	1.65	18	39
7	1:20	0.6	1.01	2	13
8	0:1	1.4	1.01	4	5

[a]Reaction condition: 0.1 mmol diester, 0.1 mmol diol, prepolymerization at 80 °C for 3 days, then polymerization in vacuum for 2 days. [b]The M_w and Đ were determined by SEC using THF as the solvent. [c]DP refer to average degree of polymerization.

After successful preparation of poly(*N*-Cbz-L-Asp-(1,8-octanediol)) ester, we expanded the substrate scope to prepare various chiral polyesters containing L-Asp. First, a series of diols with a different number of carbon atoms (from 2 to 12) were selected. As shown in Table 2, most diols were successfully polymerized to provide targeting chiral polyesters with molecular weights from 9.8 × 10^3 to 39.5 × 10^3 g/mol (M_w), except glycol. It seems to be that the chain length of diols has a significant influence on the condensation between Asp diesters and diols. According to the investigation, condensation of glycol offers the lowest molecular weight of targeting chiral polyester (0.7 × 10^3 g/mol, entry 1, Table 2). With the increasing number of carbon atoms of diols (from 2 to 8), condensation results become much better. The best condensation result can be observed when 1,8-octal diol is adopted (entry 4, Table 2). However, continuously increasing the number of carbon atoms cannot bring a better condensation result (entry 4 vs entry 5, Table 2). We believe that steric hindrance is the key factor. Taking glycol as an example, its shorter chain length probably resulted in the large steric hindrance between two -Asp units, thus polymerization was failed. For long chain diol such as dodecane-1,12-diol, the flexibility of diol chain might make this chain easy to curl and also decrease the possibility of interaction between hydroxyl and the acyl−enzyme complex, thus leading to a lower molecular weight of the obtained polymer.

Table 2. Polymerization of L-Asp Diester and Diols[a]

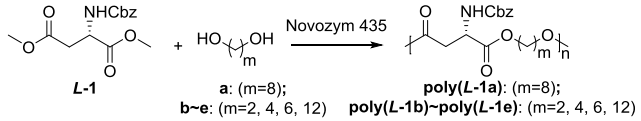

L-1 a: (m=8); b~e: (m=2, 4, 6, 12) poly(*L*-1a): (m=8); poly(*L*-1b)~poly(*L*-1e): (m=2, 4, 6, 12)

entry	*m*	M_w (×10^3 g/mol)	Đ	DP[a]	yield (%)
1	2 (**b**)	0.8	1.03	2	3
2	4 (**c**)	9.8	1.29	30	43
3	6 (**d**)	12.8	1.29	37	45
4	8 (**a**)	39.5	1.64	105	76
5	12 (**e**)	16.9	1.45	39	62

[a]See Table 1.

Next, nine L-Asp diesters with aromatic, aliphatic, and heteroatomic *N*-substitutional groups were tested. Results are listed in Table 3. The structure of *N*-substitutional groups in L-Asp diesters showed significant influence on the polymerization results. Large *N*-substitutional groups without acyl, such as −Bn and −thiophene, are favorable for the polymerization of L-Asp diesters and 1,8-octal diol, providing corresponding chiral polyesters with high molecular weight (entries 1−2, Table 3). What surprised us was the unsuccessful polycondensation of some *N*-acyl-L-Asp diesters (entry 3−7, Table 3). Acyl *N*-substitutional groups such as -propionyl, -hexanoyl were not favorable for the polymerization, and only low-molecular-weight oligomers were obtained with low yields. However, when *N*-Boc-L-Asp diester was applied, the corresponding poly(*N*-Boc-L-Asp-(1,8-octanediol)) ester with a molecular weight of up to 14.7 × 10^3 g/mol (M_w) and 75% yield was obtained successfully (entry 8, Table 3). When using -Glu as the monomer, Novozym 435 also can catalyze the polycondensation to provide the corresponding chiral

https://dx.doi.org/10.1021/acs.biomac.0c01605
Biomacromolecules 2021, 22, 918−926

Table 3. Polymerization of Various *N*-Substitutional Asp Diesters and Octanediol[a]

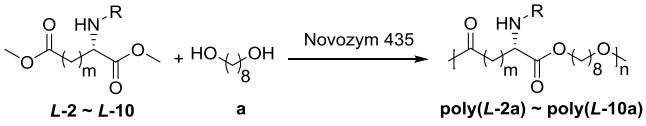

entry	R	m	M_w (×10^3 g/mol)	Đ	yield (%)
1	-Bn (***L*-2**)	1	12.1	1.49	82
2	-2-methyl-thiophene (***L*-3**)	1	11.4	1.52	87
3	-propionyl (***L*-4**)[b]	1	1.5	1.04	25
4	-hexanoyl (***L*-5**)	1	1.5	1.26	10
5	-trifluoroacetyl (***L*-6**)[b]	1	2.2	1.08	18
6	-isobutyryl (***L*-7**)	1	1.2	1.38	15
7	-pivaloyl (***L*-8**)	1	3.4	1.54	24
8	-Boc (***L*-9**)	1	14.7	1.62	75
9	-Cbz (***L*-10**)	2	19.3	1.44	86

[a]See Table 1. [b]Diethyl ester.

polyesters with a molecular weight of up to 19.3 × 10^3 g/mol (M_w) and 86% yield (entry 9, Table 3).

According to the analysis of acyl *N*-substitutional groups, it was found that bulky acyl *N*-substitutional groups like *N*-Boc and *N*-Cbz were more favorable for this polymerization than small ones. This interesting phenomenon was relative to the specific structure of *N*-substitutional Asp diesters and Novozym 435 catalytic polymerization mechanism. There were three acyl groups in acyl *N*-substitutional Asp diesters including *α*-, *β*-, and *N*-acyl. In the Novozym 435-catalyzed transesterification or polymerization process, the formation of the acyl−enzyme complex is a critical step before the nucleophilic attack of hydroxyl, which will further form a new ester bond.[15] For those *N*-acyl L-Asp diesters with small acyl groups, three acyl groups have the equal possibility to be attacked by Ser105 of Novozym 435 to form the acyl−enzyme complex. Hydroxyl of diols can efficiently attack the acyl−enzyme complex formed from *α*- and *β*-acyl of Asp diesters to make new esters bonds and further provide the targeting polymers. However, when *N*-acyl groups bind to the active site of Novozym 435 to form the acyl−enzyme complex, the esterification of hydroxyl groups of diols will be stopped because of the lower nucleophilicity of hydroxyl than amine. This process probably hinders the further polymerization. Indeed, these *N*-acyl L-Asp diesters only provided low-molecular-weight polyesters. However, bulky acyl N-substitutional groups like *N*-Boc and *N*-Cbz probably cannot bind into the active site of Novozym 435 and form the corresponding acyl−enzyme complex, thus avoid disturbing the continuous transesterification between diols and *α*- or *β*-acyl of Asp diesters.

Next, we must face how to prepare the targeting D-configurational polyester from the slow-reacting D-Asp diesters under the catalysis of Novozym 435. Generally, directed evolution or site-specific mutagenesis was a powerful tool for changing the enantioselectivity of enzymes;[16] however, it was complicated and difficult for chemists. We believe that the steric hindrance of the *α*-acyl in D-Asp diester and the corresponding lipase's selectivity limitation should be much larger than that of *β*-acyl in D-Asp diester, because of its' shorter distance to the chiral center. The transesterification between *α*-acyl in D-Asp diester and hydroxyls in diols catalyzed by Novozym 435 was probably unfavorable, thus caused the stop of chain elongation. To overcome this shortage, we designed *N*-Boc-D-*α*-octanediol-*β*-methyl-aspartate (**D-11**) as the starting monomer. Interestingly, Novozym 435-catalyzed polycondensation of **D-11** successfully provided the targeting D-configurational polyester with a molecular weight of 23.1 × 10^3 g/mol (M_w) and 68% yield (entry 2, Table 4). Moreover, we also compared another starting monomer containing 1,8-octal diol at the *β*-acyl, namely, *N*-Boc-D-*α*-methyl-*β*-octanediol-aspartate (**D-12**), although its' polycondensation also provided the corresponding polyester, but with lower molecular weight than that of **D-11** (entry 2 vs 3, Table 4). The polymerization results of **D-11** and **D-12** implied that simple substrate engineering by hiding the chiral center of the unfavorable enantiomeric monomer, thus to provide a nonchiral condensation environment artificially can efficiently overcome the selectivity limitation of enzymes.

The thermal stability of these chiral polyesters was analyzed by TG and the results are shown in Figure 1A. *N*-substitutional group in the side chains and the configuration of Asp monomers have an important influence on the thermal stability of chiral polyesters. Among these tested polyesters, **poly(L-1a)** with -Cbz *N*-substitutional group has the best thermal stability, with the weight loss less than 10% at 300 °C. And for the polyesters with similar molecular weights, the thermal stability sequence of the *N*-substitutional group was Cbz > thiophene > Bn > Boc. Indeed, **poly(D-9a)** and **poly(L-9a)** with -Boc *N*-substitutional group have the maximal weight loss ranging from 30 to 34% at 300 °C, and the temperatures at 5% weight loss ($T_{5\%}$) of **poly(D-9a)** and **poly(L-9a)** were the lowest in these tested polyesters (Table S1). By comparison, **poly(L-9a)** was slightly more thermal stable than **poly(D-9a)**. Moreover, two decomposition steps were observed in the TGA curves of **poly(L-2a)**, **poly(L-3a)**, **poly(L-9a)**, and **poly(D-9a)**, with temperatures of the maximal rate of decomposition ($T_{d\text{-}max1}$ and $T_{d\text{-}max2}$) ranging from 250 to 285 and 398 to 400

Table 4. Synthesis of D-Configurational Polyesters[a]

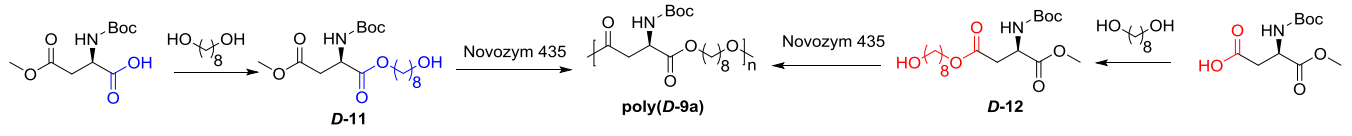

entry	monomer	polymer	M_w (×10^3 g/mol)	Đ	DP[b]	yield (%)
1	L-**9** + octanediol	**Poly(L-9a)**	14.7	1.62	40	75
2	D-**11**	**Poly(D-9a)**	23.1	2.09	65	68
3	D-**12**	**Poly(D-9a)**	6.6	1.37	17	55

[a]Syntheses of octanediol−aspartate hydroxyesters and corresponding polymers are shown in the Experimental Section. [b]See Table 1.

https://dx.doi.org/10.1021/acs.biomac.0c01605
Biomacromolecules 2021, 22, 918−926

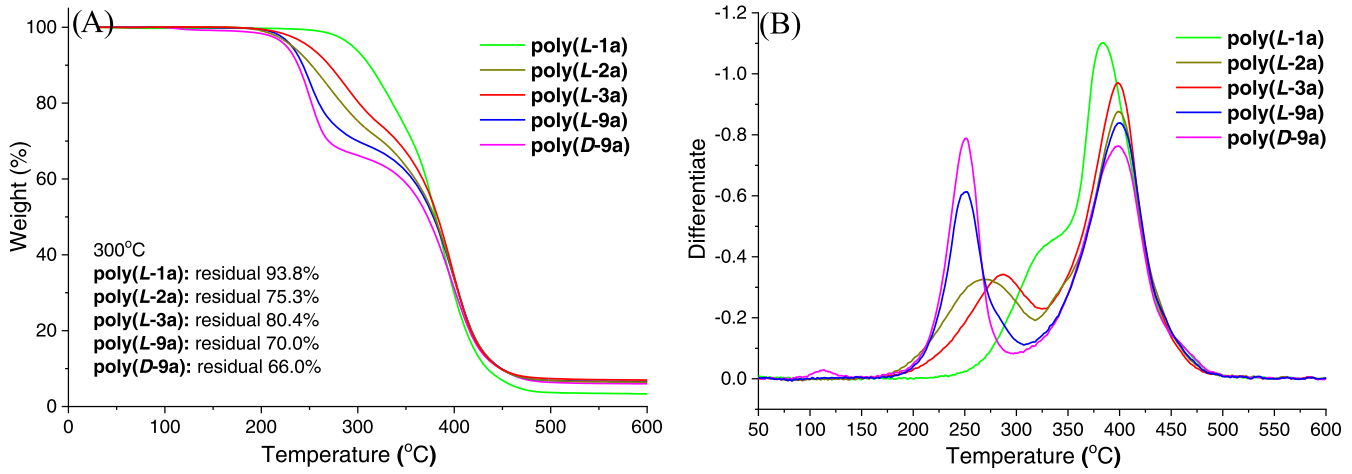

Figure 1. (A) TGA traces of chiral polyesters **poly**(L-**1a**), **poly**(L-**2a**), **poly**(L-**3a**), **poly**(L-**9a**), and **poly**(D-**9a**), weight (%) as a function of temperature (°C); (B) first derivative curves of TGA traces of polyesters **poly**(L-**1a**), **poly**(L-**2a**), **poly**(L-**3a**), **poly**(L-**9a**), and **poly**(D-**9a**). The decomposition temperature was determined at the inflection points of these curves.

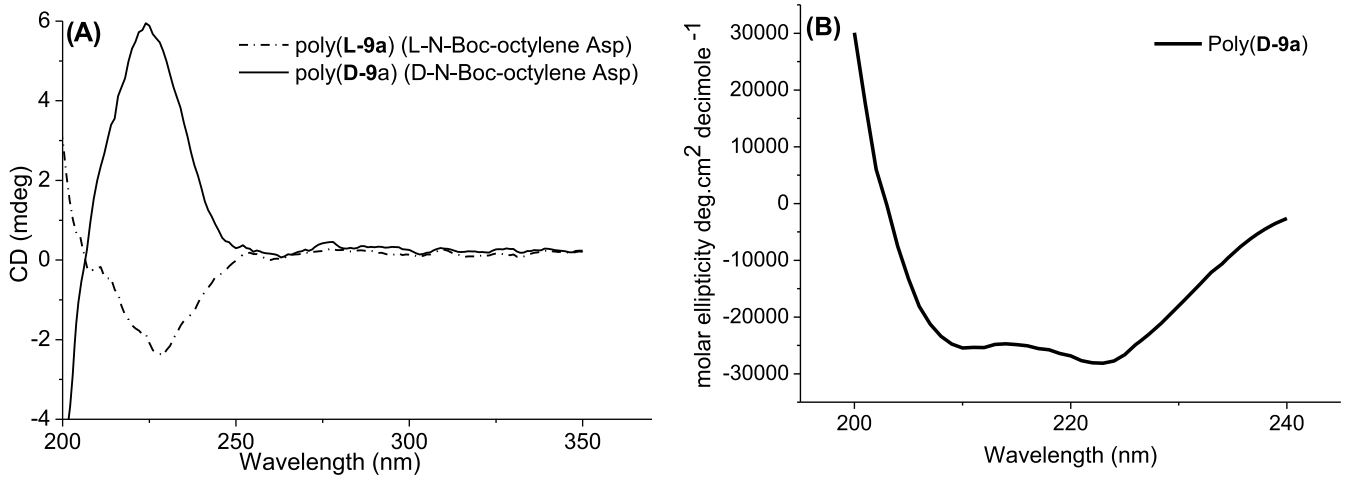

Figure 2. (A) CD spectra of **Poly**(L-**9a**) and **Poly**(D-**9a**) in acetonitrile; (B) CD analysis of **Poly**(D-**9a**), double minima at 210 and 225 nm reveal the high helical content.

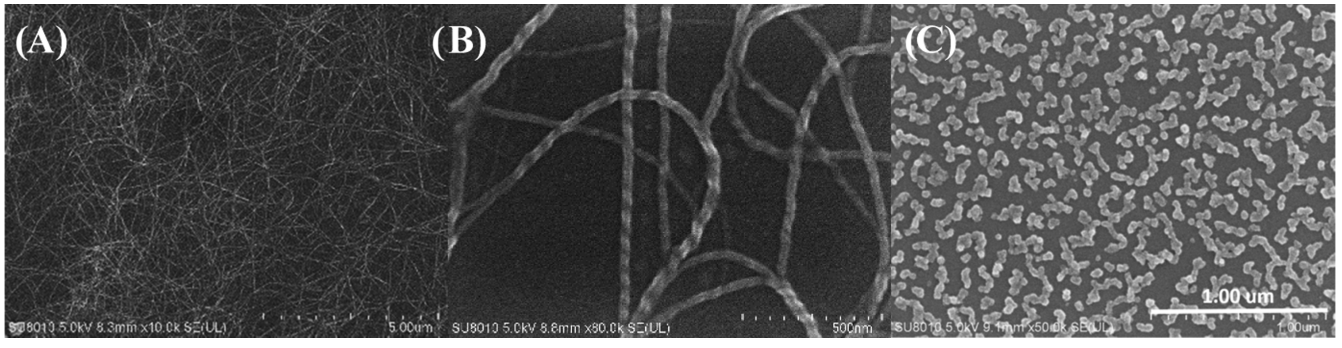

Figure 3. SEM (A–B) images of the **poly**(L-**9a**) aggregate prepared from 0.5 mg/mL solution using the solvent ratio of hexane/dichloromethane = 2:1; (C) SEM image of the mixture of **poly**(L-**9a**) and **poly**(D-**9a**) prepared under the same condition.

°C (Figure 1B), respectively, which probably related to the decomposition of *N*-substitutional group in the side chains.

Circular dichroism (CD) spectroscopy was applied to investigate the conformation and chiroptical properties of these polymers, as shown in Figure 2A. It clearly showed that D- and L-configurational polyesters produced a mirror image of negative and positive CD signals at 225 nm. Moreover, molar ellipticity curves appeared double minima at 207 and 220 nm, indicating the helix structure to be present in these chiral polyesters (Figure 2B).[17] Helix structure in the aggregate morphology of these chiral polyesters was also observed in the scanning electron microscope (SEM) images, as shown in Figure 3A,B using **poly**(L-**9a**) as one example. When the poor solvent such as hexane was added into the solution of **poly**(L-**9a**) in dichloromethane or other good solvents, fibrous aggregates with the helix structure were easily formed. Helix

https://dx.doi.org/10.1021/acs.biomac.0c01605
Biomacromolecules 2021, 22, 918–926

diameter and pitch were about 60 and 63 nm (Figure S1), respectively. Interestingly, the mixture of **poly(L-9a)** and **poly(D-9a)** formed some small aggregates with size of about 50−100 nm under the same preparation conditions (Figure 3C). The structure of *N*-substitutional groups and the configuration of the chiral Asp motif had little effect on the aggregate morphology. All tested chiral polyesters formed the similar fibrous aggregate structure (Figure S2).

To highlight the molecular basis of the formed helix microstructure of these prepared chiral polyesters, we performed Gaussian calculation of **poly(L-9a)** using Molecular Mechanics methods and UFF force field.[18] In short, we compared four different molecular arrangements of the dimer of L-**9a** and the oligomer with 10 repeating units, including parallel strands and intertwined strands (Figure S3). Initially, the dimer of L-**9a** was chosen as model, and two kinds of arrangement were compared (parallel vs convolution, Figure S3A vs Figure S3B). Computation result indicated that the electron energy of the parallel form (0.19692831 au, form A, Figure S3A) was higher than convolution forms (0.19317087, 0.18495238 and 0.19364559 au, form B−D, Figure S3B−D). The difference of form B, C, and D was the relative position of side chains in the two chain systems. For form B, side chains were in the same position. But for form C and D, the side chains were interlaced. Moreover, in form C the direction of two chains was same and in form D the direction was inverse. Among these dimers, it seemed that form C was the best arrangement of **Poly(L-9a)** with the lowest energy (Table 5).

Table 5. Electron Energy for Different Molecular Arrangements of Poly(L-9a)[a]

arrangement forms[b,c]	electron energy (au)	arrangement forms[b,d]	electron energy (au)
A	0.19 692 831	E	0.87 080 212
B	0.19 317 087	F	0.86 741 582
C	0.18 495 238	G	0.84 237 096
D	0.19 365 459	H	0.78 595 790

[a]Electron energy was calculated by Gaussian 09. [b]Sequence numbers of different arrangement forms are shown in Figure S3. [c]Dimers. [d]Oligomer with ten repeating units.

But when the repeating units were increased to 10, the results changed a lot (Figure S3E−H, forms E−H, Table 5). Among all of the arrangements in the polymer, two strands that were intertwined but oriented in the opposite direction had the lowest energy (0.78595790 au, Figure S3H, form H, Table 5), implying that the similar helix structure was probably the most stable.

CONCLUSIONS

In conclusion, Novozym 435-catalyzed polycondensation of *N*-substitutional L- or D-ASP diesters and diols to prepare enantiocomplementary chiral polyesters with high molecular weight was developed. In this polymerization, Novozym 435 showed high preference for L-enantiomer; as a result, the L-configurational chiral polyesters containing various diol chain lengths and *N*-substitutional groups were easily synthesized starting from the corresponding L-aspartate diesters and diols. It was found that bulky acyl *N*-substitutional groups like *N*-Boc and *N*-Cbz were more favorable for this polymerization than small ones such as propionyl, hexanoyl, and so on, probably due to competitively binding of these acyl groups into the active site of Novozym 435. The highest molecular weight of L-configurational chiral polyesters can reach up to 39.5×10^3 g/mol (M_w) when using L-*N*-Cbz-Asp $(OMe)_2$ as monomers. Moreover, when using slow-reacting D-aspartate diesters or racemic monomers as starting materials, only oligomers were obtained. We further demonstrated to overcome the limitations of the selectivity of Novozym 435 for the slow-reacting D-Asp diesters by modifying D-Asp diester structure to create a nonchiral condensation environment artificially, thus chiral polyesters of D-Asp with high molecular weight were also prepared successfully. These chiral polyesters are thermally stable, and *N*-substitutional groups and the configuration of Asp monomers have an important influence on their stability. CD spectra and SEM images suggested that these chiral polyesters have a helical structure with helix diameter and pitch of about 60 and 63 nm, respectively. The helical structure formed from chiral polyesters was also confirmed to be stable by Gaussian calculation. The strategy of substrate engineering to remove the selectivity limitations of lipase in polymerization will be more facile and efficient than complicated protein engineering and will be important for the future development of chiral polymer synthesis.

ASSOCIATED CONTENT

Supporting Information

The Supporting Information is available free of charge at https://pubs.acs.org/doi/10.1021/acs.biomac.0c01605.

Atomic force microscopy (AFM) analysis of **poly(L-9a)**; SEM images of chiral polyester; NMR spectra of monomers and polymers; and SEC of all chiral polyesters (PDF)

AUTHOR INFORMATION

Corresponding Authors

Qi Wu − *Department of Chemistry, Zhejiang University, Hangzhou 310027, People's Republic of China;* orcid.org/0000-0001-9386-8068; Email: wuqi1000@163.com

Bo Xia − *Jiyang College of Zhejiang A&F University, Zhuji 311800, People's Republic of China*; Email: bobohao424@126.com

Authors

Yu Zhang − *Department of Chemistry, Zhejiang University, Hangzhou 310027, People's Republic of China*

Yanyan Li − *Department of Chemistry, Zhejiang University, Hangzhou 310027, People's Republic of China*

Xianfu Lin − *Department of Chemistry, Zhejiang University, Hangzhou 310027, People's Republic of China*

Complete contact information is available at: https://pubs.acs.org/10.1021/acs.biomac.0c01605

Author Contributions

[§]Y.Z. and B.X. contributed equally to this work

Funding

Financial support from the National Natural Science Foundation of China (91956128, 21574113). Natural Science Foundation of Zhejiang province, China (LY19B020014, LY17B040002)

Notes

The authors declare no competing financial interest.

REFERENCES

(1) (a) Okamoto, Y.; Nakano, T. Asymmetric Polymerization. *Chem. Rev.* **1994**, *94*, 349−372. (b) Li, J.; Liu, Y.; Ren, W. M.; Lu, X. B. Enantioselective Terpolymerization of Racemic and Meso-epoxides with Anhydrides for Preparation of Chiral Polyesters. *Proc. Natl. Acad. Sci. U.S.A.* **2020**, *117*, 15429−15436. (c) Xu, P.; Gao, L.; Cai, C.; Lin, J.; Wang, L.; Tian, X. Helical Toroids Self-Assembled from a Binary System of Polypeptide Homopolymer and its Block Copolymer. *Angew. Chem., Int. Ed.* **2020**, *17*, 14281−14285. (d) Wan, Z.-Q.; Longo, J. M.; Chen, H. Y.; Hou, G. J.; Yang, S.; Coates, G. W.; Lu, X. B.; Liang, L. X.; Zhang, W. P. Comprehensive Understanding of Polyester Stereocomplexation. *J. Am. Chem. Soc.* **2019**, *141*, 14780−14787. (e) D'Alterio, M. C.; De Rosa, C.; Talarico, G. Stereoselective Lactide Polymerization: the Challenge of Chiral Catalyst Recognition. *ACS Catal.* **2020**, *10*, 2221−2225. (f) Mishra, S.; Mondal, A. K.; Smolinsky, E. Z. B.; Naaman, R.; Maeda, K.; Nishimura, T.; Taniguchi, T.; Yoshida, T.; Takayama, K.; Yashima, E. Spin Filtering Along Chiral Polymers. *Angew. Chem., Int. Ed.* **2020**, *59*, 14671−14676. (g) Zhang, Y.; Xia, B.; Hu, Y. J.; Zhu, Q. Y.; Lin, X. F.; Wu, Q. Enantiocomplementary Chiral Polyhydroxyenoate: Chemoenzymatic Synthesis and Helical Structure Control. *ACS Macro Lett.* **2019**, *8*, 1188−1193. (h) Xia, B.; Zhang, Y.; Zhu, Q. Y.; Lin, X. F.; Wu, Q. Enzymatic Synthesis and Stereocomplex Formation of Chiral Polyester Containing Long-Chain Aliphatic Alcohol Backbone. *Biomacromolecules* **2019**, *20*, 3584−3591.

(2) (a) Radano, C. P.; Baker, G. L.; Smith, M. R. Stereoselective Polymerization of a Racemic Monomer with a Racemic Catalyst: Direct Preparation of the Polylactic Acid Stereocomplex from Racemic Lactide. *J. Am. Chem. Soc.* **2000**, *122*, 1552−1553. (b) Chen, B.; Deng, J. P.; Yang, W. T. Hollow Two-Layered Chiral Nanoparticles Consisting of Optically Active Helical Polymer/Silica: Preparation and Application for Enantioselective Crystallization. *Adv. Funct. Mater.* **2011**, *21*, 2345−2350. (c) Banno, M.; Yamaguchi, T.; Nagai, K.; Kaiser, C.; Hecht, S.; Yashima, E. Optically Active, Amphiphilic Poly(meta-phenylene ethynylene)s: Synthesis, Hydrogen-Bonding Enforced Helix Stability, and Direct AFM Observation of Their Helical Structures. *J. Am. Chem. Soc.* **2012**, *134*, 8718−8728. (d) Liu, Y.; Wang, M.; Ren, W. M.; Xu, Y. C.; Lu, X. B. Crystalline Hetero-Stereocomplexed Polycarbonates Produced from Amorphous Opposite Enantiomers Having Different Chemical Structures. *Angew. Chem., Int. Ed.* **2015**, *54*, 7042−7046. (e) Nakano, K.; Hashimoto, S.; Nakamura, M.; Kamada, T.; Nozaki, K. Stereocomplex of Poly (propylene carbonate): Synthesis of Stereogradient Poly (propylene carbonate) by Regio- and Enantioselective Copolymerization of Propylene Oxide with Carbon Dioxide. *Angew. Chem., Int. Ed.* **2011**, *50*, 4868−4871. (f) Longo, J. M.; DiCiccio, A. M.; Coates, G. W. Poly (propylene succinate): A New Polymer Stereocomplex. *J. Am. Chem. Soc.* **2014**, *136*, 15897−15900. (g) Auriemma, F.; De Rosa, C.; Di Caprio, M. R.; Di Girolamo, R.; Ellis, W. C.; Coates, G. W. Stereocomplexed Poly (Limonene Carbonate): A Unique Example of the Cocrystallization of Amorphous Enantiomeric Polymers. *Angew. Chem., Int. Ed.* **2015**, *54*, 1215−1218.

(3) (a) Behabtu, N.; Kralj, S. Enzymatic Polymerization Routes to Synthetic−Natural Materials: A Review. *ACS Sustainable Chem. Eng.* **2020**, *8*, 9947−9954. (b) Ma, Z.; Cunningham, A. J.; Zhu, X. X. Enzymatic Conversion of Galactose Polymers into Copolymers Containing Galactonic Acid by Glucose Oxidase. *Biomacromolecules* **2020**, *21*, 2268−2275. (c) Mekonnen, T. H.; Behabtu, N.; Lenges, C. Enzymatic Polymerization Derived Engineered Polysaccharides as Reinforcing Fillers of Ethylene Vinyl acetate Composites. *Carbohydr. Polym.* **2020**, *241*, 116252−116265. (d) Lang, K.; Bhattacharya, S.; Ning, Z.; Sánchez-Leija, R. J.; Bramson, M. T. K.; Centore, R.; Corr, D. T.; Linhardt, R. J.; Gross, R. A. Enzymatic Polymerization of Poly(glycerol-1,8-octanediol-sebacate): Versatile Poly(glycerol sebacate) Analogues that Form Monocomponent Biodegradable Fiber Scaffolds. *Biomacromolecules* **2020**, *21*, 3197−3206. (e) Figueiredo, P. R.; Almeida, B. C.; Dourado, D. F. A. R.; Sousa, A. F.; Silvestre, A. J. D.; Carvalho, A. T. P. Enzymatic Synthesis of Poly(caprolactone): A QM/MM Study. *ChemCatChem* **2020**, *12*, 4845−4852.

(4) (a) Shoda, S.; Uyama, H.; Kadokawa, J.; Kimura, S.; Kobayashi, S. Enzymes as Green Catalysts for Precision Macromolecular Synthesis. *Chem. Rev.* **2016**, *116*, 2307−2413. (b) Gross, R. A.; Ganesh, M.; Lu, W. H. Enzyme-catalysis Breathes New Life into Polyester Condensation Polymerizations. *Trends Biotechnol.* **2010**, *28*, 435−443. (c) Fodor, C.; Golkaram, M.; Woortman, A. J. J.; van Dijken, J.; Loos, K. Enzymatic Approach for the Synthesis of Biobased Aromatic−Aliphatic Oligo-/polyesters. *Polym. Chem.* **2017**, *8*, 6795−6805. (d) Jiang, Y.; Woortman, A. J. J.; van Ekenstein, G. O. R. A.; Loos, K. Environmentally Benign Synthesis of Saturated and Unsaturated Aliphatic Polyesters via Enzymatic Polymerization of Biobased Monomers Derived from Renewable Resources. *Polym. Chem.* **2015**, *6*, 5451−5463. (e) Liu, B.; Zhang, X.; Chen, Y.; Yao, Z.; Yang, Z.; Gao, D.; Jiang, Q.; Liu, J.; Jiang, Z. Enzymatic Synthesis of Poly(ω-pentadecalactone-co-butylene-co-3,3′-dithiodipropionate) Copolyesters and Self-assembly of the PEGylated Copolymer Micelles as Redox-responsive Nanocarriers for Doxorubicin Delivery. *Polym. Chem.* **2015**, *6*, 1997−2010. (f) Japu, C.; de Ilarduya, A. M.; Alla, A.; Jiang, Y.; Loos, K.; Muñoz-Guerra, S. Copolyesters Made from 1,4-Butanediol, Sebacic Acid, and *d*-Glucose by Melt and Enzymatic polymerization. *Biomacromolecules* **2015**, *16*, 868−879. (g) Jiang, Y.; Woortman, A. J. J.; van Ekenstein, G. O. R. A.; Petrovic′, D. M.; Loos, K. Enzymatic Synthesis of Biobased Polyesters Using 2,5-Bis-(hydroxymethyl)furan as the Building Block. *Biomacromolecules* **2014**, *15*, 2482−2493. (h) Casajus, H.; Tranchimand, S.; Wolbert, D.; Nugier-Chauvin, C.; Cammas-Marion, S. Optimization of Lipase-catalyzed Polymerization of Benzyl Malolactonate through a Design of Experiment Approach. *J. Appl. Polym. Sci.* **2016**, *134*, No. 44604. (i) Casajus, H.; Dubreucq, E.; Tranchimand, S.; Perrier, V.; Nugier-Chauvin, C.; Cammas-Marion, S. Lipase-Catalyzed Ring-Opening Polymerization of Benzyl Malolactonate: An Unusual Mechanism? *Biomacromolecules* **2020**, *21*, 2874−2883.

(5) Duxbury, C. J.; Hilker, I.; de Wildeman, S. M. A.; Heise, A. Enzyme-Responsive Materials: Chirality to Program Polymer Reactivity. *Angew. Chem., Int. Ed.* **2007**, *46*, 8452−8454.

(6) Yeniad, B.; Naik, H.; Amir, R.; Koning, C. E.; Hawker, C. J.; Heise, A. Encoded Dendrimers with Defined Chiral Composition via 'Click' Reaction of Enantiopure Building Blocks. *Chem. Commun.* **2011**, *47*, 9870−9872.

(7) Xiao, Y.; Cummins, D.; Palmans, A. R. A.; Koning, C. E.; Heise, A. Synthesis of Biodegradable Chiral Polyesters by Asymmetric Enzymatic Polymerization and Their Formulation into Microspheres. *Soft Matter* **2008**, *4*, 593−599.

(8) Kazlauskas, R. J.; Weissfloch, A. N. E.; Rappaport, A. T.; Cuccia, L. A. A Rule to Predict Which Enantiomer of a Secondary Alcohol Reacts Faster in Reactions Catalyzed by Cholesterol Esterase, Lipase from Pseudomonas Cepacia, and Lipase from Candida Rugosa. *J. Org. Chem.* **1991**, *56*, 2656−2665.

(9) (a) van Buijtenen, J.; van As, B. A. C.; Meuldijk, J.; Palmans, A. R. A.; Vekemans, J. A. J. M.; Hulshof, L. A.; Meijer, E. W. Chiral Polymers by Iterative Tandem Catalysis. *Chem. Commun.* **2006**, 3169−3171. (b) Zhou, J. X.; Wang, W. X.; Thurecht, K. J.; Villarroya, S.; Howdle, S. M. Simultaneous Dynamic Kinetic Resolution in Combination with Enzymatic Ring-Opening Polymerization. *Macromolecules* **2006**, *39*, 7302−7305. (c) van As, B. A. C.; van Buijtenen, J.; Mes, T.; Palmans, A. R. A.; Meijer, E. W. Iterative Tandem Catalysis of Secondary Diols and Diesters to Chiral Polyesters. *Chem. - Eur. J.* **2007**, *13*, 8325−8332. (d) Kanca, Ü.; Van Buijtenen, J.; Van As, B. A. C.; Korevaar, P. A.; Vekemans, J. A. J. M.; Palmans, A. R. A.; Meijer, E. W. Iterative Tandem Catalysis of Racemic AB Monomers. *J. Polym. Sci., Part A: Polym. Chem.* **2008**, *46*, 2721−2733.

(10) van As, B. A. C.; van Buijtenen, J.; Heise, A.; Broxterman, Q. B.; Verzijl, G. K. M.; Palmans, A. R. A.; Meijer, E. W. Chiral Oligomers by Iterative Tandem Catalysis. *J. Am. Chem. Soc.* **2005**, *127*, 9964−9965.

(11) Hilker, I.; Rabani, G.; Verzijl, G. K. M.; Palmans, A. R. A.; Heise, A. Chiral Polyesters by Dynamic Kinetic Resolution Polymerization. *Angew. Chem., Int. Ed.* **2006**, *45*, 2130−2132.

https://dx.doi.org/10.1021/acs.biomac.0c01605
Biomacromolecules 2021, 22, 918−926

(12) (a) Um, P. J.; Drueckhammer, D. G. Dynamic Enzymatic Resolution of Thioesters. *J. Am. Chem. Soc.* **1998**, *120*, 5605−5610. (b) Koszelewski, D.; Brodzka, A.; Żądło, A.; Paprocki, D.; Trzepizur, D.; Zysk, M.; Ostaszewski, R. Dynamic Kinetic Resolution of 3-Aryl-4-pentenoic Acids. *ACS Catal.* **2016**, *6*, 3287−3292.
(13) (a) Verho, O.; Bäckvall, J. E. Chemoenzymatic Dynamic Kinetic Resolution: a Powerful Tool for the Preparation of Enantiomerically Pure Alcohols and Amines. *J. Am. Chem. Soc.* **2015**, *137*, 3996−4009. (b) Wu, Q.; Soni, P.; Reetz, M. T. Laboratory Evolution of Enantiocomplementary Candida antarctica Lipase B Mutants with Broad Substrate Scope. *J. Am. Chem. Soc.* **2013**, *135*, 1872−1881. (c) Xia, B.; Cheng, G. L.; Lin, X. F.; Wu, Q.; Li, Y. Lipase-Catalyzed Doubly Enantioselective Ring-Opening Resolution between Alcohols and Lactones: Synthesis of Chiral Hydroxyl Esters with Two Stereogenic Centers. *ChemCatChem* **2014**, *6*, 3448−3454. (d) Champagne, E.; Strandman, S.; Zhu, X. X. Recent Developments and Optimization of Lipase-Catalyzed Lactone Formation and Ring-Opening Polymerization. *Macromol. Rapid Commun.* **2016**, *37*, 1986−2004. (e) Xia, B.; Xu, J.; Xiang, Z. W.; Cen, Y. X.; Hu, Y. J.; Wu, Q.; Lin, X. Stereoselectivity-Tailored, Metal-Free Hydrolytic Dynamic Kinetic Resolution of Morita-Baylis-Hillman Acetates Using an Engineered Lipase-Organic Base Cocatalyst. *ACS Catal.* **2017**, *7*, 4542−4549.
(14) Zhang, Y.; Xia, B.; Li, Y. Y.; Wang, Y. Y.; Lin, X. F.; Wu, Q. Solvent-Free Lipase-Catalyzed Synthesis: Unique Properties of Enantiopure D- and L- Polyaspartates and Their Complexation. *Biomacromolecules* **2016**, *17*, 362−370.
(15) Bornscheuer, U. T.; Kazlauskas, R. J. *Hydrolases in Organic Synthesis: Regio- and Stereoselective Biotransformations*, 2nd ed.; Wiley-VCH, 2005.
(16) (a) Reetz, M. T. Laboratory Evolution of Stereoselective Enzymes: A Prolific Source of Catalysts for Asymmetric Reactions. *Angew. Chem., Int. Ed.* **2011**, *50*, 138−174. (b) Renata, H.; Wang, Z. J.; Arnold, F. H. Expanding the Enzyme Universe: Accessing Non-Natural Reactions by Mechanism-Guided Directed Evolution. *Angew. Chem., Int. Ed.* **2015**, *54*, 3351−3367.
(17) (a) Maroun, R. G.; Krebs, D.; Antri, S. E.; Deroussent, A.; Fermandjian, S.; et al. Self-association and Domains of Interactions of an Amphipathic Helix Peptide Inhibitor of HIV-1 Integrase Assessed by Analytical Ultracentrifugation and NMR Experiments in Trifluoroethanol/H_2O Mixtures. *J. Biol. Chem.* **1999**, *274*, 34174−34185. (b) Marshall, C. B.; Chakrabartty, A.; Davies, P. L. Hyperactive Antifreeze Protein from Winter Flounder Is a Very Long Rod-like Dimer of α-Helices. *J. Biol. Chem.* **2005**, *280*, 17920−17929. (c) Chen, Y. X.; Guarnieri, M. T.; Vasil, A. I.; Vasil, M. L.; Mant, C. T.; Hodges, R. S. Role of Peptide Hydrophobicity in the Mechanism of Action of Alpha-helical Antimicrobial Peptides. *Antimicrob. Agents Chemother.* **2007**, *51*, 1398−1406. (d) Duncan, K. A.; Huber, S. C. Sucrose Synthase Oligomerization and F-actin Association are Regulated by Sucrose Concentration and Phosphorylation. *Plant Cell Physiol.* **2007**, *48*, 1612−1623. (e) Ronzone, E.; Wesolowski, J.; Bauler, L. D.; Bhardwaj, A.; Hackstadt, T.; Paumet, F. An α-Helical Core Encodes the Dual Functions of the Chlamydial Protein IncA. *J. Biol. Chem.* **2014**, *289*, 33469−33480.
(18) (a) Frisch, M. J.; Trucks, G. W.; Schlegel, H. B.; Scuseria, G. E.; Robb, M. A.; Cheeseman, J. R.; Scalmani, G.; Barone, V.; Mennucci, B.; Petersson, G. A. et al. *Gaussian 09*, revision D.01; Gaussian Inc: Wallingford, CT, 2009. (b) Rappe, A. K.; Casewit, C. J.; Colwell, K. S.; Goddard, W. A.; Skiff, W. M. UFF, a Full Periodic Table Force Field for Molecular Mechanics and Molecular Dynamics Simulations. *J. Am. Chem. Soc.* **1992**, *114*, 10024−10035.

https://dx.doi.org/10.1021/acs.biomac.0c01605
Biomacromolecules 2021, 22, 918−926